AIChE

Nonbuoyancy Density-Driven Convective Mass and Heat Transfer: Scaling Analysis and Solution Methodology

William B. Krantz
Singapore Membrane Technology Center, Nanyang Technological University, Singapore 639798

Hanyong Lee, Siladitya Ray Chaudhuri, and Sun-Tak Hwang
Dept. of Chemical & Materials Engineering, University of Cincinnati, Cincinnati, OH 45221

DOI 10.1002/aic.12631

Density change during mass or heat transfer can cause convection in the absence of buoyancy forces. Prior studies have shown that this convection can be significant in the determination of diffusion coefficients and in the casting of polymeric membranes. Including this effect is challenging even for advanced numerical codes. A general methodology for obtaining the mass-average velocity for unsteady-state, one-dimensional, multicomponent mass and/or heat transfer circumvents the problem of numerically solving the coupled continuity equation. Scaling analysis permits assessing the importance of this convection for a generic equation-of-state. Numerical predictions for evaporation from a liquid layer for components having density ratios of 1:1 and 0.7:1 indicate that ignoring convection results in errors of 34% and 24% in the evaporation time and final thickness, respectively. This convection also influences the evaporation in the percutaneous application of cosmetics, medications, and insecticides, curing of paints, varnishes, and lacquers, and formation of thin films. © 2011 American Institute of Chemical Engineers *AIChE J,* 58: 678–689, 2012

Keywords: diffusion (mass transfer, heat transfer), heat transfer, mass transfer, mathematical modeling, transport

Introduction

Many applications involving mass and/or heat transfer are accompanied by significant densification or dilation owing to the dependence of the mass density on concentration or temperature. These density changes can cause convection even in the absence of buoyancy forces. A methodology for incorporating this convection induced by density change and assessing its importance are the focus of this article. Note that throughout this article the terminology ‘‘convection induced by density change’’ will refer to bulk flow generated in the absence of any buoyancy forces.

Convection induced by density change can be important in applications involving mass and/or heat transfer even in the absence of buoyancy forces. These applications can involve concentration and/or temperature gradients that in turn can give rise to significant convection generated by density change. Examples include the solvent-casting of polymeric membranes and thin films, application of cosmetics, ointments, medications, and insect repellants to the skin, and the drying of paints, lacquers, and other surface coatings. Describing the mass and/or heat transfer in applications such as these is complex. For an m-component system a set of coupled, unsteady-state, nonlinear, partial differential equations must be solved involving the continuity equation for

---

Correspondence concerning this article should be addressed to W. B. Krantz at krantz@colorado.edu.

the overall mass, $m-1$ species-balance equations and the thermal energy equation. In addition, an equation-of-state is needed for the overall mass density as a function of the $m-1$ concentrations, temperature and pressure. If either mass loss/gain or density change is involved, boundary conditions must be applied at a moving interface whose location is unknown. Hence, an auxiliary condition involving an integral mass balance is required to locate this moving boundary. Mass- and/or heat-transfer problems of this type are particularly challenging to solve even with the most advanced numerical codes.

The problem associated with convection induced by density change has been addressed in several ways. The simplest approach has been to ignore this convection in the hope that it is not significant; this is equivalent to assuming equi-mass counter-diffusion for a binary system in mass-transfer applications. If the volume-of-mixing is essentially zero, another approach in mass-transfer applications has been to assume that the volume-average velocity is zero and to express Fick's law of diffusion in terms of mass fluxes relative to the volume-average velocity. However, for one-dimensional (1-D) mass and/or heat transfer, it is possible to develop an integral equation for the mass-average velocity that decouples solving the continuity equation along with the species-conservation and/or thermal energy equations. This equation for the mass-average velocity can be incorporated into the $m-1$ species-balance and/or thermal energy equations, which then can be solved via well-established numerical methods.

The organization of this article is as follows. First, a brief review is given of prior studies that have addressed convection induced by density change in the absence of any buoyancy forces. The generalized equation for determining the mass-average velocity for unsteady-state, 1-D, multicomponent mass and/or heat transfer then is developed. The describing equations are subsequently developed for a special case of unsteady-state, 1-D, mass transfer, namely evaporation and densification or dilation of a liquid layer containing a volatile and a nonvolatile component. These describing equations then are scaled to determine the criteria for assessing when convection induced by density change is significant. The describing equations then are solved numerically to illustrate the error that can be encountered in predicting the instantaneous concentration profiles, mass-average velocity and liquid layer thickness when convection induced by density change is ignored. The conclusions emanating from this study then are summarized. The details of the systematic scaling analysis are given in the Appendix.

Prior Studies

There have been relatively few modeling studies that have incorporated convection induced by density change owing to mass and/or heat transfer in the absence of buoyancy forces. Duda and Vrentas[1] showed that an integral equation could be developed for the mass-average velocity for any 1-D mass-transfer problem for which the mass density was a function only of concentration. They then corrected the results of binary diffusion experiments for the effect of a nonzero volume-of-mixing. They found that small changes in volume could result in large errors in the calculated values of the diffusion coefficients. No attempt was made to provide a general assessment of the error encountered when convection owing to density change is neglected. Moreover, convection arising from thermally induced density changes was not considered.

Tan et al.[2] were the first to identify the importance of convection induced by density change in the absence of buoyancy forces for the multicomponent mass transfer involved in evaporative polymeric membrane casting. However, their equation for the mass-average velocity is in error.

Tsay and McHugh[3] also considered multicomponent mass transfer in evaporative polymeric membrane casting. They used an equation-of-state based on Flory-Huggins theory that implied that the volume-of-mixing and correspondingly the volume-average velocity was identically zero. They then formulated the species-balance equations in terms of mass fluxes relative to the volume-average velocity. Their approach avoids having to explicitly account for any convective effects owing to density change since they are implicitly incorporated into the diffusive fluxes in their describing equations. However, this approach is valid only for an equation-of-state for which the volume-of-mixing is zero. Moreover, this approach does not permit assessing the importance of the convection arising from density change since it is implicitly incorporated into the diffusive flux terms.

Bardow et al.[4] considered convection in a mixture while trying to measure diffusion coefficients in a concentrated solution whose density was markedly concentration-dependent. They used an algorithm proposed by Unger et al.[5] that uses Boolean algebra to perform index analysis on systems of differential-algebraic equations and developed an expression for the mass-average velocity. Although they do not show the derivation of the equation for the mass-average velocity, it presumably was the same as that developed by Duda and Vrentas.[1] They do not develop any criteria for assessing when convection induced by density change is important.

Lee et al.[6] allowed for the effect of convection induced by density change in a model they developed for the evaporative casting of polymeric membranes via phase inversion. The describing equations for evaporative casting of a ternary system requires solving the unsteady-state, 1-D, coupled continuity, species-balance, and thermal energy equations incorporating concentration- and temperature-dependent physical and transport properties, and applying boundary conditions at a moving interface. This system of equations could not be solved via any numerical code because of the coupling with the continuity equation. Hence, they used the approach of Duda and Vrentas[1] to develop an explicit equation for the mass-average velocity, thereby obviating the need to numerically solve the continuity equation. Their model predictions for the cellulose-acetate/acetone/water system indicated that the convective contribution to the mass-transfer flux can be 35% of that due to diffusion during the early stages of evaporative casting. Moreover, their model agreed much better with the measurements of Shojaie et al.[7] for the instantaneous solution mass and surface temperature than did the same model in the absence of convection induced by density change that was developed by Shojaie et al.[8] They concluded that this convective flux contribution can have a marked effect on the properties of the functional layer of asymmetric membranes that is formed at the upper surface early in the casting process. They made no attempt to assess the criteria for when this convection effect is important. Moreover, they could not determine the importance of the convective flux contribution at long times since their model is not applicable after phase separation occurs.

In a later paper Lee et al.[9] incorporated convection induced by density change in a model they advanced for the wet-casting of polymeric membranes via phase inversion. The describing equations involved solving the unsteady-state, 1-D, coupled continuity and species-balance equations incorporating concentration-dependent physical and transport properties, and applying boundary conditions at a moving interface. Hence, they again used the approach of Duda and Vrentas[1] to obtain an explicit equation for the mass-average velocity for unsteady-state, 1-D, multicomponent mass transfer. Their predictions for the cellulose acetate/acetone/water system indicated that convection induced by density change was even more pronounced than for evaporative casting of the same system. Densification-induced convection can increase the mass-transfer flux by nearly two orders-of-magnitude shortly after initiating wet-casting. Hence, the convective flux contribution will have an even greater influence on the properties of the functional layer of wet-cast membranes. Including convection induced by density change in their model allowed them to explain the effect of the initial casting solution thickness on the propensity to form undesirable macrovoid pores. Pekny et al.[10,11] showed that a substantial supersaturated (i.e., within the metastable two-phase region of the ternary phase diagram) region near the interface of the casting solution is necessary for macrovoid pore formation. A substantial supersaturated region was predicted by Lee et al. for a 125 μm but not for a 75 μm initial casting solution thickness. Moreover, a supersaturated region was not predicted by Lee et al. for the 125 μm initial casting solution thickness when convection induced by density change was not included in the model. The densification-induced velocity retards the loss of solvent (acetone) but aids the influx of nonsolvent (water) during wet casting. This effect, in combination with the ability of the thicker casting solution to provide solvent from depth, delays crossing rapidly into the two-phase region thereby facilitating supersaturation. No attempt was made to develop any criteria for assessing the importance of convection arising from density change. Again they could not assess the importance of convection induced by density change at long times since their model is not applicable once phase separation occurs.

This brief review indicates that the convection generated by density change in the absence of any buoyancy-induced body forces has been shown to significantly affect mass-transfer processes such as determining diffusion coefficients in concentrated solutions and fabricating polymeric membranes. In particular, Lee et al.[6,9] demonstrated that densification-induced convection can have a dramatic effect on the casting of polymeric membranes. However, these prior efforts to include convection induced by density change were ad hoc in that specific equations-of-state were used for the concentration-dependence of the density. Interestingly, there appear to be no attempts to address the problem of convection induced by density change in the absence of buoyancy forces that can arise owing to temperature changes. No prior studies appear to have developed the criteria needed to assess the importance of convection induced by density change. An assessment also needs to be made of the error that can be encountered when this convection induced by density change is ignored. The long time behavior of the convection induced by density change needs to be studied to determine whether it has an influence throughout the mass-transfer process. Addressing these needs then constitutes the goal of the research reported in this article.

Generalized Equation for the Mass-Average Velocity Arising from Density Change

Here we follow the approach of Duda and Vrentas[1] to develop an equation for the mass-average velocity induced by density change. However, Duda and Vrentas considered only solutally induced density changes, whereas here we generalize their approach to include thermally induced density changes. The continuity, species-balance and thermal energy equations are given by

$$\frac{\partial \rho}{\partial t} = -\rho \frac{\partial w}{\partial z} - w \frac{\partial \rho}{\partial z} \tag{1}$$

$$\frac{\partial \rho_i}{\partial t} = -\frac{\partial n_i}{\partial z} = -\frac{\partial}{\partial z}(j_i + w\rho_i) \quad \text{for} \quad i = 1, 2, \ldots m-1 \tag{2}$$

$$\rho \frac{\partial e}{\partial t} + \rho w \frac{\partial e}{\partial z} = -\frac{\partial q}{\partial z} - P \frac{\partial w}{\partial z} \tag{3}$$

Where t and z are the temporal and spatial coordinates, respectively, ρ is the mass density, ρ_i is the mass concentration, n_i is the mass flux relative to a stationary observer, j_i is the mass flux relative to the mass-average velocity w, m denotes the number of components in the multicomponent mixture, $e \equiv C_v T$ is the internal energy per unit mass where T is the temperature, C_v is the heat capacity at constant volume, q is the heat flux, and P is the pressure. Equations 1–3, when combined with appropriate equations for the mass and heat fluxes, constitute $m + 2$ unknowns in $m + 1$ equations (ρ, w, the $m-1$ mass concentrations ρ_i, and T). An additional equation is required, which constitutes an equation-of-state for the density written formally as

$$\rho = \rho(T, P, \rho_1 \ldots \rho_{m-1}) \tag{4}$$

Equations 1–4 require specifying initial and boundary conditions appropriate to the particular mass- and/or heat-transfer problem. If mass loss/gain and/or densification/dilation are occurring, one or more of the boundary conditions must be applied at a moving interface. To specify the location of any moving boundary, an auxiliary condition is required, which is obtained via an integral mass balance. Solving a coupled nonlinear system of equations involving a moving boundary is challenging even for the most advanced numerical codes. However, the coupling with the continuity equation can be avoided using the approach outlined here.

The first step in this methodology involves rearranging Eq. 1 while allowing for the concentration and temperature dependence of the density as follows:

$$\frac{\partial w}{\partial z} = -\frac{1}{\rho}\frac{\partial \rho}{\partial t} - \frac{w}{\rho}\frac{\partial \rho}{\partial z} = -\sum_{i=1}^{m-1}\left(\frac{\partial \rho_i}{\partial t} + w\frac{\partial \rho_i}{\partial z}\right)\frac{1}{\rho}\frac{\partial \rho}{\partial \rho_i} - \left(\frac{\partial e}{\partial t} + w\frac{\partial e}{\partial z}\right)\frac{1}{\rho}\frac{\partial \rho}{\partial e} \tag{5}$$

The density in Eq. 5 has been expressed as a function of $m-1$ species concentrations ρ_i and the internal energy per unit mass e rather than the temperature. This has been done because the thermal energy equation is expressed in terms of e. After an explicit equation for the mass-average velocity w has been developed, it will be recast in terms of the temperature.

Combining Eqs. 2, 3, and 5 and solving for $\frac{\partial w}{\partial z}$ gives the following:

$$\frac{\partial w}{\partial z} = \frac{\sum\limits_{i=1}^{m-1} \frac{\partial \rho}{\partial \rho_i} \frac{\partial j_i}{\partial z}}{\rho - \sum\limits_{i=1}^{m-1} \rho_i \frac{\partial \rho}{\partial \rho_i}} + \frac{\frac{\partial \rho}{\partial e} \frac{\partial q}{\partial z}}{\rho^2 - P \frac{\partial \rho}{\partial e}} \tag{6}$$

Integrate Eq. 6 to obtain an explicit equation for w, the mass-average velocity:

$$w = \int\limits_0^z \left[\frac{\frac{\partial \rho}{\partial e} \frac{\partial q}{\partial \tilde{z}}}{\rho^2 - P \frac{\partial \rho}{\partial e}} + \sum_{i=0}^{m-1} \frac{\frac{\partial \rho}{\partial \rho_i}}{\rho - \rho_i \frac{\partial \rho}{\partial \rho_i}} \frac{\partial j_i}{\partial \tilde{z}} \right] d\tilde{z} \tag{7}$$

where $\tilde{z}$ denotes a dummy integration variable. In integrating Eq. 6 the lower boundary has been assumed to be impermeable, although this assumption is not critical to the analysis. An alternate form of Eq. 7 can be obtained that is more convenient when the mass density is expressed in terms of the mass fraction and the temperature by using the chain rule of differentiation to obtain the following:

$$w = \int\limits_0^z \frac{1}{\rho^2} \left[\frac{\frac{\partial \rho}{\partial T} \frac{\partial q}{\partial z}}{\left(C_v + T \frac{\partial C_v}{\partial T} \right) - \frac{P}{\rho^2} \frac{\partial \rho}{\partial T}} + \sum_{i=0}^{m-1} \frac{\partial \rho}{\partial \omega_i} \frac{\partial j_i}{\partial \tilde{z}} \right] d\tilde{z} \tag{8}$$

Equations 7 and 8 permit determining the instantaneous local mass-average velocity if an equation-of-state is known for the mass density as a function of concentration and/or temperature. Equations 7 and 8 are general results for 1-D unsteady-state mass and/or heat transfer and can be applied to multicomponent as well as binary systems when appropriate equations are substituted for the fluxes.

The methodology leading to Eqs. 7 and 8 is limited in that it assumes 1-D heat, mass and momentum transfer. This precludes using these equations when multidimensional effects such as free convection are involved. It clearly is necessary to solve the 1-D species-balance and/or thermal energy equation to obtain the concentrations, temperature, and mass and heat fluxes. It might also be necessary to solve the 1-D equation-of-motion to obtain the pressure if the latter depends on the velocity. The utility of this methodology is that it obviates the need to solve the species-balance and/or energy equation coupled with the continuity equation, which can be challenging for even the most sophisticated numerical codes.

Scaling Describing Equations for Evaporative Mass Transfer from a Liquid Layer

As an example of unsteady-state 1-D mass transfer for which density change can cause convection, consider the isothermal evaporation of a liquid film containing a volatile and a nonvolatile component denoted by 1 and 2, respectively, as shown in Figure 1. The origin of the coordinate system is placed on the moving interface to accommodate a scaling that encompasses both short and long times. This requires the coordinate transformation $z = L(t) - \hat{z}$ where z is a spatial coordinate measured from the fixed lower impermeable boundary and $\hat{z}$ is a spatial coordinate measured from the moving interface between the liquid film and ambient gas phase. At short times the mass transfer will be confined to a solutal boundary layer that penetrates downward from the upper interface. At longer times this solutal boundary layer will penetrate to the lower boundary. A generic equation-of-state for the mass density of a binary system as a function of the temperature, pressure and mass fraction of one of the components is written formally as follows:

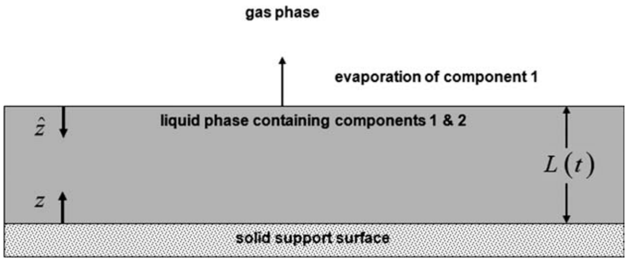

Figure 1. Schematic of the evaporation of a liquid layer containing a volatile and a nonvolatile component showing coordinate systems referenced to fixed lower impermeable boundary and referenced to moving upper interface between liquid film and ambient gas phase.

$$\rho = \rho(T, P, \omega_1) \tag{9}$$

Since the goal of this scaling analysis is to assess when convection generated by a solutally induced density change becomes important, it is sufficient to consider only small departures of the density from its initial value denoted here by ρ_0. Hence, we can expand Eq. 9 in a Taylor series for small departures of the mass fraction of component 1 from its initial value ω_{10}:

$$\rho = \rho|_{\omega_{10}} + \left. \frac{\partial \rho}{\partial \omega_1} \right|_{\omega_{10}} (\omega_1 - \omega_{10}) + \mathrm{O}(\omega_1 - \omega_{10})^2$$
$$\cong \rho_0 - \beta(\omega_1 - \omega_{10}) \tag{10}$$

Where $\beta \equiv -\left. \frac{\partial \rho}{\partial \omega_1} \right|_{\omega_{10}}$; the negative sign is introduced so that $\beta > 0$ when densification occurs owing to a decrease in ω_1. Assuming small departures of the concentration from its initial value in no way limits this scaling analysis since if density-induced convection is found to be important for small changes in the concentration, it most certainly will be significant for large changes.

For a binary system one needs to consider the continuity equation and a species balance for one of the two components. The species-balance equation given by Eq. 2 for volatile component 1 in a coordinate system referenced to the moving interface simplifies to the following:

$$\rho\frac{\partial\omega_1}{\partial t}+\rho\frac{dL}{dt}\frac{\partial\omega_1}{\partial\hat{z}}+\rho w\frac{\partial\omega_1}{\partial\hat{z}}=-\frac{\partial j_1}{\partial\hat{z}} \tag{11}$$

The transformation to a coordinate system located on the interface introduces a pseudo-convection term that is proportional to the velocity of the moving boundary. In Eq. 11 j_1 is the mass flux relative to the mass-average velocity given by Fick's law of diffusion:

$$j_1=-D_{12}\frac{\partial(\omega_1\rho)}{\partial\hat{z}} \tag{12}$$

Where D_{12} is the binary diffusion coefficient for components 1 and 2, which is assumed to be constant; this assumption is not critical to the analysis. The solution to the continuity equation is given by Eq. 8, which for an isothermal system simplifies to the following for the concentration dependence of the density given by Eq. 10 and a coordinate system located at the upper interface as shown in Figure 1:

$$w=\int_0^{\hat{z}}\frac{1}{\rho^2}\frac{\partial\rho}{\partial\omega_1}\frac{\partial j_1}{\partial\tilde{z}}d\tilde{z}=-\int_0^{\hat{z}}\frac{\beta}{[\rho_0-\beta(\omega_1-\omega_{10})]^2}\frac{\partial j_1}{\partial\tilde{z}}d\tilde{z}\cong-\frac{\beta}{\rho_0^2}j_1 \tag{13}$$

When Eqs. 11 and 12 are combined, we obtain a nonlinear second-order partial differential equation that requires an initial and two boundary conditions. The boundary conditions are given by

$$j_1=0 \quad \text{at} \quad \hat{z}=L \tag{14}$$

$$j_1=-k_G\alpha_G\omega_1(1-\omega_1) \quad \text{at} \quad \hat{z}=0 \tag{15}$$

Where k_G is the mass-transfer coefficient for the evaporative mass transfer into the gas phase at the upper interface and α_G is the distribution coefficient that interrelates the mass fractions of component 1 in the liquid and gas phases at the upper interface. Equation 14 merely states that the lower solid boundary is impermeable; a permeable lower boundary can easily be incorporated into the analysis. Equation 15 is the result of an integral mass balance on component 1 over the entire liquid layer for which a lumped parameter description of the evaporative mass transfer of component 1 at the upper surface has been used. Since Eq. 14 is applied at a moving boundary (in a coordinate system attached to the moving liquid-gas interface), an auxiliary condition is needed to determine its location. This is obtained from an integral balance on the total mass in the liquid layer and is given by

$$\rho\frac{dL}{dt}+\rho w=-k_G\alpha_G\omega_1 \quad \text{at} \quad \hat{z}=0 \tag{16}$$

The initial conditions needed to solve Eqs. 11 and 16 are given by the following:

$$\omega_1=\omega_{10}, \quad L=L_0 \quad \text{at} \quad t=0 \tag{17}$$

Where ω_{10} and L_0 are the initial mass fraction of component 1 and liquid film thickness, respectively.

A systematic scaling analysis will be done on the describing equations given by 10–17 using the procedure outlined by Deen[12] (pp. 74–91) and discussed in detail by Krantz.[13] This differs from conventional dimensional analysis in that all the dimensionless dependent and independent variables as well as the temporal and spatial derivatives are bounded to be o(1) (little "oh" of one). By this we mean that their magnitude can range from zero to ~1. The dimensionless groups emerging from a systematic scaling analysis permit assessing the relative importance of the various terms in the describing equations. Here we seek to determine the importance of the convection terms generated by a density change.

The systematic scaling analysis of the describing equations will only be outlined here. More details are provided in the Appendix. We begin by introducing the following dimensionless variables:

$$\omega^*\equiv\frac{\omega_1}{\omega_{1\mathrm{s}}};\ \rho^*\equiv\frac{\rho}{\rho_{\mathrm{s}}};\ w^*\equiv\frac{w}{w_{\mathrm{s}}};\ t^*\equiv\frac{t}{t_{\mathrm{s}}};$$
$$\hat{z}^*\equiv\frac{\hat{z}}{\hat{z}_{\mathrm{s}}};\ j_1^*\equiv\frac{j_1}{j_{1\mathrm{s}}};\ L^*\equiv\frac{L}{L_{\mathrm{s}}};\ \left(\frac{dL}{dt}\right)^*\equiv\frac{1}{\dot{L}}\frac{dL}{dt} \tag{18}$$

Where $\omega_{1s},\rho_s,w_s,t_s,\hat{z}_s,j_{1s},L_s$ and $\dot{L}_s$ are unspecified scale factors for the mass fraction of component 1, mass density, mass-average velocity, time, spatial coordinate, mass flux with respect to the mass-average velocity, instantaneous liquid film thickness, and time-rate of change of the liquid film thickness, respectively. Systematic scaling differs from conventional dimensional analysis in that it is often necessary to scale derivatives to bound them to be o(1) as has been done for the time-rate of change of the liquid film thickness. These unspecified scale factors will be determined by setting appropriate dimensionless groups equal to one to achieve o(1) scaling. These dimensionless groups are generated by substituting the dimensionless variables into the describing equations and dividing through each equation by the dimensional coefficient of one term. This procedure, which is described in detail in the Appendix, results in the following scale factors:

$$\begin{aligned}
&\omega_{1\mathrm{s}}=\omega_{10},\ \rho_{\mathrm{s}}=\rho_0,\ w_{\mathrm{s}}=\frac{\beta D_{12}\omega_{10}}{\rho_0\delta}, \quad t_{\mathrm{s}}=t_{\mathrm{c}},\\
&j_{1\mathrm{s}}=\frac{D_{12}\omega_{10}\rho_0}{\delta},\ L_{\mathrm{s}}=L_0,\ \dot{L}_{\mathrm{s}}=\frac{k_{\mathrm{G}}\alpha_{\mathrm{G}}\omega_{10}}{\rho_0}\\
&\hat{z}_{\mathrm{s}}=\delta=\sqrt{D_{12}t_{\mathrm{c}}} \quad \text{for} \quad 0\le t_{\mathrm{c}}<\frac{L^2}{D_{12}},\\
&\hat{z}_{\mathrm{s}}=L \quad \text{for} \quad \frac{L^2}{D_{12}}\le t_{\mathrm{c}}<\infty
\end{aligned} \tag{19}$$

Where the time scale t_{c} is the contact time, which can be any time at which one chooses to observe the mass-transfer process, and δ is the time-dependent solutal boundary-layer thickness whose functional form was determined by balancing the accumulation and diffusion terms in the dimensionless form of Eq. 11. Note that the length scale $\hat{z}_s$ is equal to the solutal boundary-layer thickness $\delta=\sqrt{D_{12}t_c}$ whose limiting value is the instantaneous thickness of the liquid layer L The use of scale factors such as t_{c} and δ in systematic scaling analysis is a marked departure from conventional dimensional analysis.

When these scale factors are substituted into the describing equations, they assume the following form:

$$\rho^* \frac{\partial \omega_1^*}{\partial t^*} + \omega_{10}\mathrm{Bi}_\delta \rho^* \left(\frac{dL}{dt}\right)^* \frac{\partial \omega_1^*}{\partial \hat{z}^*} + \mathrm{Pe}\rho^* w^* \frac{\partial \omega_1^*}{\partial \hat{z}^*} = -\frac{\partial j_1^*}{\partial \hat{z}^*} \quad \text{for} \quad 0 \le t_c < \frac{L^2}{D_{12}} \tag{20a}$$

$$\frac{1}{\mathrm{Fo}}\rho^* \frac{\partial \omega_1^*}{\partial t^*} + \omega_{10}\mathrm{Bi}_\mathrm{L} \rho^* \left(\frac{dL}{dt}\right)^* \frac{\partial \omega_1^*}{\partial \hat{z}^*} + \mathrm{Pe}\rho^* w^* \frac{\partial \omega_1^*}{\partial \hat{z}^*} = -\frac{\partial j_1^*}{\partial \hat{z}^*} \text{for} \frac{L^2}{D_{12}} \le t_c < \infty \tag{20b}$$

$$j_1^* = -\frac{\partial(\omega_1^* \rho^*)}{\partial \hat{z}^*} \tag{21}$$

$$\rho^* = 1 - \mathrm{Pe}(\omega_1^* - 1) \tag{22}$$

$$w^* = -j_1^* \tag{23}$$

$$j_1^* = 0 \quad \text{at} \quad \hat{z}^* = \frac{L_0}{\delta}L^* \tag{24}$$

$$j_1^* = -\mathrm{Bi}_\delta \omega_1^*(1 - \omega_{10}\omega_1^*) \quad \text{at} \quad \hat{z}^* = 0 \quad \text{for} \quad 0 \le t_c < \frac{L^2}{D_{12}} \tag{25a}$$

$$j_1^* = -\mathrm{Bi}_\mathrm{L} \omega_1^*(1 - \omega_{10}\omega_1^*) \quad \text{at} \quad \hat{z}^* = 0 \quad \text{for} \quad \frac{L^2}{D_{12}} \le t_c < \infty \tag{25b}$$

$$\rho^*\left(\frac{dL}{dt}\right)^* + \frac{1}{\omega_{10}}\frac{\mathrm{Pe}}{\mathrm{Bi}_\delta}\rho^* w^* = -\omega_1^* \quad \text{at} \quad \hat{z}^* = 0 \quad \text{for} \quad 0 \le t_c < \frac{L^2}{D_{12}} \tag{26a}$$

$$\rho^*\left(\frac{dL}{dt}\right)^* + \frac{1}{\omega_{10}}\frac{\mathrm{Pe}}{\mathrm{Bi}_\mathrm{L}}\rho^* w^* = -\omega_1^* \quad \text{at} \quad \hat{z}^* = 0 \quad \text{for} \quad \frac{L^2}{D_{12}} \le t_c < \infty \tag{26b}$$

$$\omega_1^* = 1, \quad L^* = 1 \quad \text{at} \quad t^* = 0 \tag{27}$$

Where $\mathrm{Pe} \equiv \frac{w_s \delta}{D_{12}} = \frac{\beta\omega_{10}}{\rho_0}$ is the solutal Peclet number, which is a measure of the ratio of the convection to diffusion of species. However, since the convection arises from densification or dilation (i.e., the velocity scale w_s is expressed in terms of the density change), the solutal Peclet number is a measure of the relative change in density. For this reason the solutal Peclet number also appears in the equation-of-state given by Eq. 22. $\mathrm{Fo} \equiv \frac{D_{12}t_c}{L^2}$ is the solutal Fourier number and is a measure of the ratio of the contact time to the characteristic time for diffusive mass transfer. $\mathrm{Bi}_\delta \equiv \frac{k_G \alpha_G \delta}{\rho_0 D_{12}}$ and $\mathrm{Bi}_L \equiv \frac{k_G \alpha_G L}{\rho_0 D_{12}}$ are solutal Biot numbers at the upper interface based on δ and L, respectively, as the characteristic length. The solutal Biot number is a measure of the ratio of the overall mass transfer into the gas phase to the diffusive mass transfer within the liquid layer.

We now can use the results of our scaling analysis to assess the importance of convection caused by density changes and to determine when various approximations are possible. The criterion for ignoring the effect of convection induced by density change in the species-balance equation given by Eqs. 20a,b is determined by the following:

$$\mathrm{Pe} = \frac{\beta\omega_{10}}{\rho_0} \ll 1 \quad \text{for} \quad 0 \le t_c < \infty \tag{28}$$

If Pe = O(1) (big "oh" of one), which implies that it is approximately equal to one, the convection term must be retained in Eqs. 20a,b. Note that the group Pe is proportional to the ratio of the velocity scale w_s to the diffusive mass-flux scale j_s. This implies that the characteristic convection velocity is equal to the product of Pe and the characteristic diffusive mass-flux scale. An interesting consequence of this observation from scaling analysis is that if Pe $\cong$ 1, the resulting convection will be just as important as diffusion throughout the entire mass-transfer process.

However, even if Pe $\ll$ 1, the convection induced by density change can influence the mass-transfer process through the auxiliary condition used to determine the instantaneous location of the interface. Hence, this latter effect will influence the ability to satisfy the overall conservation of mass given by Eqs. 26a,b, which are the result of an integral mass balance. The criterion for this latter effect of density change to be negligible is the following:

$$\frac{1}{\omega_{10}}\frac{\mathrm{Pe}}{\mathrm{Bi}_\delta} = \frac{\beta D_{12}}{k_G \alpha_G \delta} \ll 1 \tag{29}$$

Clearly the criterion demanded by Eq. 29 might not be satisfied even when Pe $\ll$ 1 if the product $\omega_{10}\mathrm{Bi}_\delta \ll 1$. Conversely, it can still be satisfied even when Pe $\cong$ 1 if the product $\omega_{10}\mathrm{Bi}_\delta$ is sufficiently large.

The criterion for assuming quasi-steady-state mass transfer is determined by assessing when the accumulation term is negligible in Eq. 20b:

$$\mathrm{Fo} = \frac{D_{12}t_c}{L^2} \gg 1 \tag{30}$$

If the criterion given by Eq. 30 is satisfied, Eqs. 20b and 21 can be solved analytically for the spatial dependence of the mass fraction, thereby reducing the problem to solving an ordinary differential equation to determine the time dependence. This is particularly advantageous if one is seeking to develop a simple 1-D quasi-steady-state model to be used in modeling a more complex multidimensional mass-transfer process such as is done using simple film, penetration, and boundary layer models as described in Bird et al. (pp. 703–716).[14]

Although this scaling analysis was carried out to assess the importance of convection generated by densification for a mass-transfer problem, a similar scaling analysis could be done for an analogous heat-transfer problem. The conclusions regarding the importance of convection would then be recast in terms of the thermal Peclet, Fourier and Biot numbers, with the dimensional parameter characterizing the change in density now being defined as $\beta \equiv \frac{d\rho}{dT}\big|_{T_0}$, where T_0 is the initial temperature.

Presentation of Numerical Results and Discussion

To provide quantitative validation of the scaling analysis results, the describing equations were solved numerically using the D03PPF routine developed by the National Algorithms Group (NAG®) that is well-suited for solving problems for which the gradients can become very large. This numerical code uses the method-of-lines and the GEAR method for the spatial and temporal integrations, respectively.[15] The physical and transport properties, and system parameters are given in Table 1. To carry out this numerical integration, it was necessary to specify a specific equation-of-state for the mass density. This was assumed to be given by

$$\rho = \frac{\overset{\circ}{\rho}_1 \overset{\circ}{\rho}_2}{\overset{\circ}{\rho}_1 + \omega_1 \Delta \overset{\circ}{\rho}_{12}} \tag{31}$$

where $\overset{\circ}{\rho}_i$ is the mass density of pure component i and $\Delta\overset{\circ}{\rho}_{12} \equiv \overset{\circ}{\rho}_2 - \overset{\circ}{\rho}_1$. If $\Delta\overset{\circ}{\rho}_{12} > 0$, densification will occur as component 1 evaporates that will cause a mass-average velocity directed from the interface to the lower surface (a positive velocity with respect to the coordinate system located on the moving interface). If $\Delta\overset{\circ}{\rho}_{12} < 0$, dilation will occur and the mass-average velocity will be in the opposite direction. Equation 31 is an equation-of-state frequently used to describe the concentration dependence of the mass density of polymer solutions. It implies a zero volume-of-mixing and correspondingly a zero volume-average velocity. However, it does not imply a zero mass-average velocity. Although the full form of Eq. 31 was used in the numerical simulation, the Taylor series expansion of Eq. 31 is needed to identify the parameter β used in the scaling analysis; that is,

$$\rho = \frac{\overset{\circ}{\rho}_1 \overset{\circ}{\rho}_2}{\overset{\circ}{\rho}_1 + \omega_1 \Delta \overset{\circ}{\rho}_{12}} \cong \rho_0 - \frac{\rho_0^2 \Delta \overset{\circ}{\rho}_{12}}{\overset{\circ}{\rho}_1 \overset{\circ}{\rho}_2}(\omega_1 - \omega_{10}) = \rho_0 - \beta(\omega_1 - \omega_{10}) \tag{32}$$

To assess the effects of convection arising from density change, numerical simulations were carried out for two sets of conditions for the pure component densities: $\overset{\circ}{\rho}_1 = \overset{\circ}{\rho}_2 = 1$; and $\overset{\circ}{\rho}_1 = 0.7, \overset{\circ}{\rho}_2 = 1$. Since species 1 is the volatile component, densification will occur when $\overset{\circ}{\rho}_2 > \overset{\circ}{\rho}_1$. Since this is a generic example, the distribution coefficient was assumed to be equal to one. An upper bound on the binary diffusion coefficient of $D_{12} = 10^{-4}$ cm^2/s was assumed to maximize the effect of diffusion relative to any convection generated by the density change. Consequently the numerical simulation will give a conservative estimate of the effect of convection generated by density change since assuming a lower value for the diffusivity would increase the influence of convection relative to diffusion (i.e., increase the solutal Peclet number).

The physical and transport properties, and system parameters in Table 1 imply the following values for the dimensionless groups:

$$\mathrm{Pe} = 0.177 \tag{33}$$

$$0 \le \mathrm{Bi}_\delta \le 12.1 \tag{34}$$

Table 1. Physical Properties, Transport Properties, and System Parameters

Property or Parameter	Numerical Value
Binary diffusion coefficient, D_{12}	10^{-4} cm^2/s
Gas phase mass-transfer coefficient, k_G	10^{-2} g/cm^2 s
Partition coefficient, α	1.0
Pure component density of volatile species 1, ρ_1^o	0.7 or 1 g/cm^3
Pure component density of nonvolatile species 2, ρ_2^o	1 g/cm^3
Initial mass fraction of volatile species 1, ω_{10}	0.5
Initial liquid layer thickness, L_0	10^{-1} cm
Initial solution density, ρ_0	0.824 g/cm^3
Densification parameter, β	0.291 g/cm^3
Peclet number, Pe	0.117
Fourier number, Fo	$0 \le \mathrm{Fo} < \infty$
Biot number, Bi_δ	$0 \le \mathrm{Bi}_\delta \le 12.1$

$$0.029 \le \frac{1}{\omega_{10}} \frac{\mathrm{Pe}}{\mathrm{Bi}_\delta} < \infty \tag{35}$$

$$0 \le \mathrm{Fo} < \infty \tag{36}$$

Since Pe > 0, densification rather than dilation will occur and the velocity generated by this density change will be directed from the liquid-gas interface toward the lower solid boundary. The magnitude of Pe is sufficiently large to imply that convective transport will contribute significantly throughout the entire mass-transfer process. The dimensionless group $\frac{1}{\omega_{10}}\frac{\mathrm{Pe}}{\mathrm{Bi}_\delta}$ becomes unbounded as $t_c \rightarrow 0$ since the Biot number is proportional to the contact time. A systematic scaling analysis implies that every term in each of the describing equations must be bounded of o(1), Eq. 26a then implies that $w^* \rightarrow 0$ as $\frac{1}{\omega_{10}}\frac{\mathrm{Pe}}{\mathrm{Bi}_\delta} \rightarrow \infty$; that is, the dimensionless mass-average velocity generated by densification must become vanishing small at short times when $\mathrm{Bi}_\delta \rightarrow 0$. However, this does not imply that the dimensional mass-average velocity becomes small at short times; it is a consequence of the scale factor $w_s = \frac{\Delta\overset{\circ}{\rho}_{12} D_{12} \omega_{10}}{\overset{\circ}{\rho}_1 \delta}$ becoming unbounded at short times when $\delta \rightarrow 0$. Since the solutal Biot number Bi_δ can become as large as 10 at longer times when $\delta \rightarrow L$, Eq. 25b implies that $\omega^* \rightarrow \mathrm{O}(0.1)$ as $\mathrm{Bi}_\delta \rightarrow 10$ to keep the product Bi_δ ω^* bounded of o(1). The solutal Fourier number can become quite large for sufficiently long contact times, which implies that quasi-steady-state mass transfer can occur. This permits solving Eqs. 20b and 21 analytically to reduce the problem to solving an ordinary differential equation for the time dependence. In addition to the insight into the behavior of the mass-transfer process that a systematic scaling analysis provides, it also permits a more in-depth interpretation of the predictions of the numerical solution to the describing equations.

Figures 2a,b show plots of the mass-fraction profile in the liquid layer with the contact time t_c as a parameter for $\Delta\overset{\circ}{\rho}_{12} = 0.3$ and $\Delta\overset{\circ}{\rho}_{12} = 0$, respectively. In these figures the coordinate system has been referenced to the lower solid boundary to show the thinning of the liquid film that occurs due to both the evaporation of component 1 and densification. Both plots display the solutal boundary layer behavior suggested by scaling analysis; that is, the solutal boundary layer thickness grows proportional to the square-root of

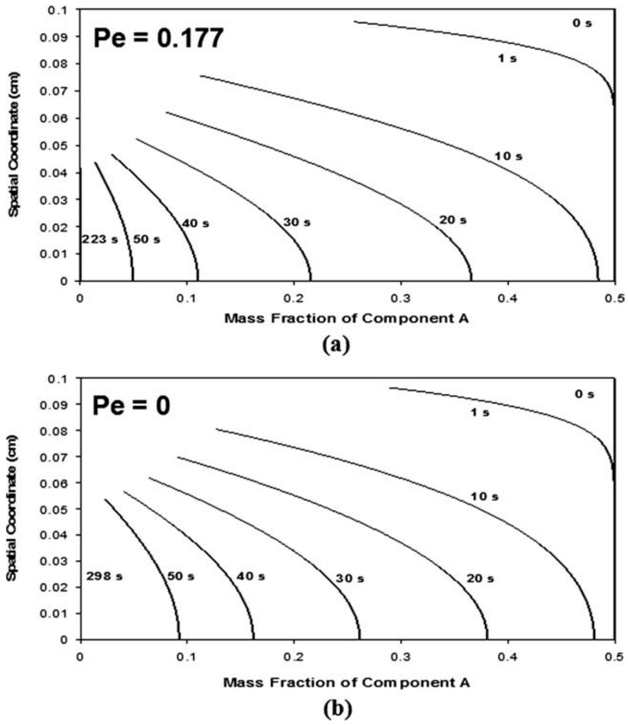

(a)

(b)

Figure 2. Model predictions for the concentration profiles for contact times ranging from zero to that required for complete evaporation of the volatile component: (a) predictions including convection arising from densification owing to a 30% difference in the pure component densities for which Pe = 0.177; (b) predictions for components having equal pure component densities for which Pe = 0 and no convention will be generated by density change.

time. However, the penetration of the solutal boundary layer is seen to be considerably more rapid in Figures 2a than in 2b. This is a consequence of the densification-induced convection aiding the diffusive penetration of the solutal boundary layer; that is, $w < 0$ (in a coordinate system located at the lower solid boundary). For this same reason complete evaporation occurs within 223 seconds in Figure 2a owing to the effect of densification-induced convection, whereas it requires 298 seconds in Figure 2b in the absence of any convection. This implies an error of 34% if the convection arising from densification is ignored in the model.

Figure 3 shows a plot of the dimensional mass-average velocity profile in the liquid layer with the contact time t_c as a parameter for $\Delta\mathring{\rho}_{12} = \mathbf{0.3}$. Again the coordinate system has been referenced to the lower solid boundary and normalized with respect to the instantaneous total thickness of the liquid layer. In this case a comparable plot for $\Delta\mathring{\rho}_{12} = \mathbf{0}$ is trivial since the mass-average velocity is zero in the absence of any density change. Note first that the mass-average velocity is negative in a coordinate system referenced to the lower boundary, thereby implying that it is directed from the liquid-gas interface towards the lower solid boundary; that is, the densification-induced convection enhances the rate of film thinning and solutal boundary-layer penetration (as shown in Figs. 2a and b). Note that the dimensional mass-average velocity w becomes quite large at the liquid-gas interface as $t_c \to 0$. However, Eq. 26a indicates that as $\mathrm{Bi}_\delta \to 0$ when $\delta \to 0$, the dimensionless mass-average velocity $w^* \to 0$ because the velocity scale $w_s \to \infty$ as t_c (i.e., δ) $\to 0$. Since Pe (i.e., the solutal Peclet number) in Eq. 20a involves the product of w_s and δ it remains bounded and equal to 0.177 throughout the evaporation process. The implication of this is that the convective transport owing to densification is just as important as diffusion throughout the entire evaporation process even at short times when the concentration gradient and associated diffusive mass transfer become extremely large.

Figure 4 shows a plot of the instantaneous thickness of the liquid layer as a function of time predicted by the full set of describing equations that incorporate densification-induced convection and predicted by the same set of equations for which convection effects are suppressed. Also shown in Figure 4 is the prediction for the final liquid layer thickness L_∞ after the evaporation of component 1 is complete. This is determined from a mass balance using Eq. 31 and is given by the following:

$$L_\infty = \frac{L_0 \omega_{20} \mathring{\rho}_1}{\omega_{10}\mathring{\rho}_2 + \omega_{20}\mathring{\rho}_1} \tag{37}$$

The model incorporating densification-induced convection predicts $L_\infty = 0.0412$ after ~75 seconds, the same value predicted by Eq. 37, which confirms the accuracy of the numerical simulation. In contrast, the same model in which the

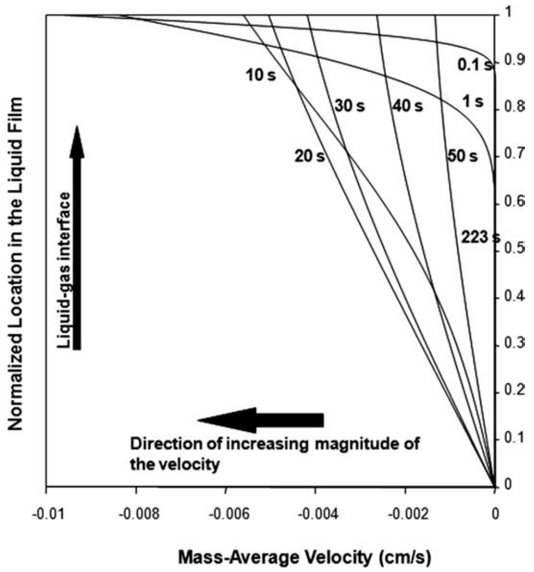

Figure 3. Model predictions for the mass-average-velocity profile for contact times ranging from zero to that required for complete evaporation of the volatile component for a 30% difference in the pure component densities for which Pe = 0.177.

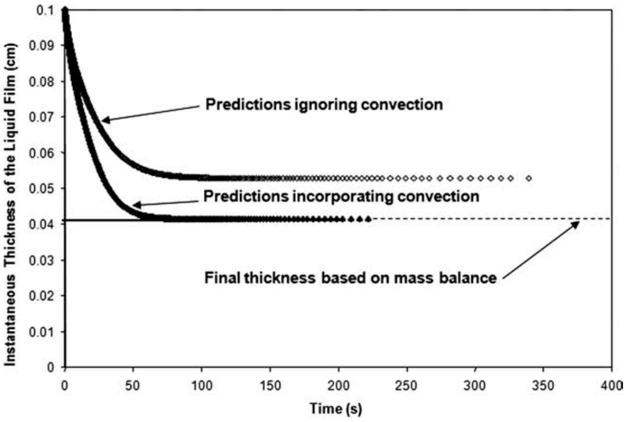

Figure 4. Model predictions for instantaneous film thickness as a function of contact time: ◆ – predictions including convection arising from densification owing to a 30% difference in pure component densities for which Pe = 0.177; ◇ – predictions for components having equal pure component densities for which Pe = 0 and no convention will be generated by density change; the dashed line shows final liquid layer thickness dictated by a mass balance.

densification-induced convection is suppressed predicts $L_\infty = 0.0525$ corresponding to a 27% error in predicting the final liquid layer thickness. This significant error incurred if the convection induced by density change is ignored is a consequence of the dimensionless group $\frac{1}{\omega_{10}}\frac{\text{Pe}}{\text{Bi}_\delta}$ in Eq. 26a becoming very large early in the evaporation process.

Conclusions

Significant convective mass transfer can arise owing to density changes in the absence of any gravitationally induced body forces. An explicit equation for the mass-average velocity generated by this convection induced by density change has been developed for unsteady-state, 1-D, multicomponent mass and/or heat transfer. This methodology obviates the need to solve the coupled continuity, species-balance and/or thermal energy equations that can be numerically challenging particularly when a moving boundary is involved. Applying this methodology only requires having an appropriate equation-of-state for the mass density as a function of concentration and/or temperature. However, this methodology is limited to 1-D mass, heat and momentum transfer. As such, it precludes applying it to multidimensional flows such as those involving free convection. A systematic scaling analysis of the describing equations for a generic mass-transfer problem involving the evaporation of the binary liquid layer led to identifying the dimensionless groups whose magnitude permitted assessing the importance of this convection effect arising from density changes. The effect of this convection on the species-balance equation is determined by the magnitude of the dimensionless group $\text{Pe} \equiv \frac{w_s\delta}{D_{12}} = \frac{\beta\omega_{10}}{\rho_0}$. Only if $\text{Pe} \ll 1$ can this convection effect be ignored in the species-balance equation. The effect of this convection on the overall mass balance is determined by the magnitude of the dimensionless group $\frac{1}{\omega_{10}}\frac{\text{Pe}}{\text{Bi}_\delta}$. Only if $\frac{1}{\omega_{10}}\frac{\text{Pe}}{\text{Bi}_\delta} \ll 1$ can this convection induced by density change be ignored in the overall mass balance. A numerical simulation of this evaporative mass-transfer problem for conditions such that the pure component densities of the two components differ by 30% indicated that ignoring this convection effect resulted in an error of 34% in predicting the time required for complete evaporation and an error of 27% in predicting the final liquid layer thickness. A particularly important conclusion from this study is that the mass-average velocity generated by density change can be very large near the interface at short contact times. If densification occurs, this velocity is antiparallel to the direction of evaporative mass transfer. As such, it causes more rapid penetration of the solutal boundary layer and thereby accelerates the rate of evaporation. Moreover, it can significantly influence the properties of the upper interface in applications such as the curing of paints varnishes, and lacquers, and can play a major role in determining the permselectivity of the functional layer of polymeric membranes fabricated via phase inversion. This convection effect induced by density change in the absence of buoyancy forces can also influence the application of cosmetics, ointments, medications, and insect repellents.

Acknowledgments

The authors gratefully acknowledge the support of this research by the NASA Microgravity Research Division (NAG3–2451).

Notation

$\text{Bi}_L = \frac{k_G\alpha_G L}{\rho_0 D_{12}}$, solutal Biot number based on L as characteristic length, dimensionless
$\text{Bi}_\delta = \frac{k_G\alpha_G \delta}{\rho_0 D_{12}}$, solutal Biot number based on δ as characteristic length, dimensionless
D_{12} = binary diffusion coefficient for components 1 and 2, $\frac{\text{cm}^2}{\text{s}}$
$\text{Fo} = \frac{D_{12}t_c}{L^2}$, solutal Fourier number, dimensionless
j_i = mass flux of component i with respect to the mass-average velocity, $\frac{\text{g}}{\text{cm}^2\cdot\text{s}}$
k_G = gas-phase mass-transfer coefficient, $\frac{\text{g}}{\text{cm}^2\cdot\text{s}}$
L = instantaneous liquid layer thickness, cm
L_0 = initial liquid layer thickness, cm
L_∞ = final liquid layer thickness, cm
$\dot{L}_s$ = scale factor for $\frac{dL}{dt}$, $\frac{\text{cm}}{\text{s}}$
m = number of components in a multicomponent mixture
n_i = mass flux of component i with respect to a fixed reference frame, $\frac{\text{g}}{\text{cm}^2\cdot\text{s}}$
P = pressure, $\frac{\text{g}}{\text{cm}\cdot\text{s}^2}$
$\text{Pe} = \frac{w_s\delta}{D_{12}} = \frac{\beta\omega_{10}}{\rho_0}$, solutal Peclet number
T = temperature, K
t = time, s
t_c = contact time, s
w = mass-average velocity, $\frac{\text{cm}}{\text{s}}$
z = spatial coordinate measured from lower impermeable surface, cm
$\hat{z}$ = spatial coordinate measured from upper moving interface, cm
$\tilde{z}$ = dummy spatial coordinate integration variable, cm

Greek letters

α_G = distribution coefficient between mass fractions in gas and liquid phases, dimensionless
$\beta = -\left.\frac{d\rho}{d\omega_1}\right|_{\omega_{10}}$, coefficient in Taylor series expansion of the mass density
$\Delta\rho_{12} = \overset{\circ}{\rho}_2 - \overset{\circ}{\rho}_1$, difference between pure component density of components 2 and 1, $\frac{\text{g}}{\text{cm}^3}$

$\delta = \sqrt{D_{12}t_c}$, solutal boundary layer thickness, cm
ρ = mass density, $\frac{\mathrm{g}}{\mathrm{cm}^3}$
ρ_i = mass concentration of component i, $\frac{\mathrm{g}}{\mathrm{cm}^3}$
$\underset{\circ}{\rho}_i$ = pure component density of component i, $\frac{\mathrm{g}}{\mathrm{cm}^3}$
ρ_0 = mass density evaluated at ω_{10}, $\frac{\mathrm{g}}{\mathrm{cm}^3}$
ω_i = mass fraction of component i, dimensionless
ω_{i0} = initial mass fraction of volatile component 1, dimensionless

Subscripts/Superscripts

i = integer denoting either volatile component 1 or nonvolatile component 2
s = denotes scale factor
1 = denotes volatile component
2 = denotes nonvolatile component
* = denotes a dimensionless variable or derivative

Literature Cited

1. Duda JL, Vrentas JS. Analysis of free diffusion experiments in binary systems. *Ind Eng Chem Fundam.* 1965;4:301–308.
2. Tan L, Krantz WB, Greenberg AR, Sani RL. Studies of convective transport in evaporative casting of dense polymer films. *J Membr Sci.* 1995;108:245–255.
3. Tsay CS, McHugh AJ. Mass transfer modeling of asymmetric membrane formation by phase inversion. *J Polym Sci Polym Phys.* 1990;28:1327–1365.
4. Bardow A, Marquardt W, Goeke V, Koss HJ, Lucas K. Model-based measurement of diffusion using Raman spectroscopy. *AIChE J.* 2003;49:323–334.
5. Unger J, Kroner A, Marquardt W. Structural analysis of differential-algebraic equation systems—theory and applications. *Comput Chem Eng.* 1995;19:867–882.
6. Lee H, Chaudhuri SR, Krantz WB, Hwang ST. A model for evaporative casting of polymeric membranes incorporating convection due to density changes. *J Membr Sci.* 2006;284:161–172.
7. Shojaie SS, Krantz WB, Greenberg AR. Dense polymer film and membrane formation via the dry-cast process part II. Model validation and morphological studies. *J Membr Sci.* 1994;94:281–298.
8. Shojaie SS, Krantz WB, Greenberg AR. Dense polymer film and membrane formation via the dry-cast process part I. Model development. *J Membr Sci.* 1994;94:255–280.
9. Lee H, Krantz WB, Hwang ST. A model for wet-casting polymeric membranes incorporating nonequilibrium interfacial dynamics, vitrification and convection. *J Membr Sci.* 2010;354:74–85.
10. Pekny MR, Greenberg AR, Khare V, Zartman J, Krantz WB, Todd P. Macrovoid pore formation in dry-cast cellulose acetate membranes: buoyancy studies. *J Membr Sci.* 2002;205:11–21.
11. Pekny MR, Zartman J, Krantz WB, Greenberg AR, Todd P. Flow-visualization during macrovoid pore formation in dry-cast cellulose acetate membranes. *J Membr Sci.* 2003;211:71–90.
12. Deen WM. *Analysis of Transport Phenomena*. New York: Oxford University Press, 1998.
13. Krantz WB. *Scaling Analysis in Modeling Transport and Reaction Processes—A Systematic Approach to Model Building and the Art of Approximation*. New York: Wiley, 2007.
14. Bird RB, Stewart WE, Lightfoot EN. *Transport Phenomena*, 2nd ed. New York: Wiley, 2007.
15. NAG Fortran Library Manual, D03PPF/D03PPA. The National Algorithms Group Inc., 2002.

Appendix: Scaling Analysis

The mass-transfer problem considered here is shown in Figure 1. At short contact times the mass transfer will be confined to a solutal boundary layer near the upper interface. Hence, it is expedient to locate the coordinate system at the interface as shown in Figure 1. The describing equations then are given by

$$\rho\frac{\partial\omega_1}{\partial t}+\rho\frac{dL}{dt}\frac{\partial\omega_1}{\partial\hat{z}}+\rho w\frac{\partial\omega_1}{\partial\hat{z}}=-\frac{\partial j_1}{\partial\hat{z}} \tag{A1}$$

$$j_1=-D_{12}\frac{\partial(\omega_1\rho)}{\partial\hat{z}} \tag{A2}$$

$$\rho=\rho|_{\omega_{10}}+\left.\frac{\partial\rho}{\partial\omega_1}\right|_{\omega_{10}}(\omega_1-\omega_{10})+\mathrm{O}(\omega_1-\omega_{10})^2\cong\rho_0-\beta(\omega_1-\omega_{10}) \tag{A3}$$

$$w=-\frac{\beta}{\rho_0^2}j_1 \tag{A4}$$

$$\omega_1=\omega_{10},\quad L=L_0\quad\text{at}\quad t=0 \tag{A5}$$

$$j_1=0\quad\text{at}\quad\hat{z}=L \tag{A6}$$

$$j_1=-k_{\mathrm{G}}\alpha_{\mathrm{G}}\omega_1(1-\omega_1)\quad\text{at}\quad\hat{z}=0 \tag{A7}$$

$$\rho\frac{dL}{dt}+\rho w=-k_G\alpha_G\omega_1\quad\text{at}\quad\hat{z}=0 \tag{A8}$$

The systematic scaling analysis used here follows the procedure outlined by Krantz.[13] It differs from conventional dimensional analysis in that it bounds each dependent and independent variable and the derivatives to be o(1); that is, they are bounded between zero and ∼1.

Introduce the following dimensionless variables involving unspecified scale factors:

$$\omega_1^*\equiv\frac{\omega_1}{\omega_{1\mathrm{s}}};\rho^*\equiv\frac{\rho}{\rho_{\mathrm{s}}};w^*\equiv\frac{w}{w_{\mathrm{s}}};t^*\equiv\frac{t}{t_{\mathrm{s}}};$$
$$\hat{z}^*\equiv\frac{\hat{z}}{\hat{z}_{\mathrm{s}}};j_1^*\equiv\frac{j_1}{j_{1\mathrm{s}}};L^*\equiv\frac{L}{L_{\mathrm{s}}};\left(\frac{dL}{dt}\right)^*\equiv\frac{1}{\dot{L}_s}\frac{dL}{dt} \tag{A9}$$

Note that the derivative $\frac{dL}{dt}$ has been given its own scale factor since there is no reason to believe that it scales as $\frac{L_s}{t_s}$. Note also that the mass fraction is also scaled even though it is dimensionless; this is to insure that ω_1^* is bounded of o(1). Substitute these dimensionless variables in Eqs. A1–A8 and divide through by the dimensional coefficient of one term in each of the describing equations. If one divides through by the dimensional coefficient of a term that must be retained in the analysis to insure physical significance, then when this term is bounded to be o(1), all the other terms, when they are properly scaled, will be o(1) as well. This results in the following set of dimensionless describing equations:

$$\frac{\rho_{\mathrm{s}}\omega_{1\mathrm{s}}\hat{z}_{\mathrm{s}}}{t_{\mathrm{s}}j_{1\mathrm{s}}}\rho^*\frac{\partial\omega_1^*}{\partial t^*}+\frac{\rho_{\mathrm{s}}\omega_{1\mathrm{s}}\dot{L}_{\mathrm{s}}}{j_{1\mathrm{s}}}\rho^*\left(\frac{dL}{dt}\right)^*\frac{\partial\omega_1^*}{\partial\hat{z}^*}+\frac{\rho_{\mathrm{s}}w_{\mathrm{s}}\omega_{1\mathrm{s}}}{j_{1\mathrm{s}}}\rho^*w^*\frac{\partial\omega_1^*}{\partial\hat{z}^*}=-\frac{\partial j_1^*}{\partial\hat{z}^*} \tag{A10}$$

$$j_1^*=-\frac{D_{12}\omega_{1\mathrm{s}}\rho_{\mathrm{s}}}{\hat{z}_{\mathrm{s}}j_{1\mathrm{s}}}\frac{\partial(\omega_1^*\rho^*)}{\partial\hat{z}^*} \tag{A11}$$

$$\rho^*=\frac{\rho_0}{\rho_{\mathrm{s}}}-\frac{\beta\omega_{1\mathrm{s}}}{\rho_{\mathrm{s}}}\left(\omega_1^*-\frac{\omega_{10}}{\omega_{1\mathrm{s}}}\right) \tag{A12}$$

$$w^* = -\frac{\beta j_{1s}}{\rho_0^2 w_s} j_1^* \tag{A13}$$

$$\omega_1^* = \frac{\omega_{10}}{\omega_{1s}}, \quad L^* = \frac{L_0}{L_s} \quad \text{at} \quad t^* = 0 \tag{A14}$$

$$j_1^* = 0 \quad \text{at} \quad \hat{z}^* = \frac{L_s}{\hat{z}_s} L^* \tag{A15}$$

$$j_1^* = -\frac{k_G \alpha_G \omega_{1s}}{j_{1s}} \omega_1^* \left(1 - \omega_{1s}\omega_1^*\right) \quad \text{at} \quad \hat{z}^* = 0 \tag{A16}$$

$$\rho^* \left(\frac{dL}{dt}\right)^* + \frac{w_s}{\dot{L}_s} \rho^* w^* = -\frac{k_G \alpha_G \omega_{1s}}{\rho_s \dot{L}_s} \omega_1^* \quad \text{at} \quad \hat{z}^* = 0 \tag{A17}$$

The scale factors now are determined by setting appropriate dimensionless groups equal to one to bound all the variables and derivatives to be o(1); this implies that the variable or derivative is bounded between zero and ∼1. The scales for ρ^*, ω_1^*, and L^* are determined by setting the dimensionless groups appearing in Eqs. A12 and A14 equal to one:

$$\frac{\omega_{10}}{\omega_{1s}} = 1 \Rightarrow \omega_{1s} = \omega_{10} \tag{A18}$$

$$\frac{\rho_s}{\rho_0} = 1 \Rightarrow \rho_s = \rho_0 \tag{A19}$$

$$\frac{L_0}{L_s} = 1 \Rightarrow L_s = L_0 \tag{A20}$$

Since the mass loss is determined principally by the evaporation at the interface, the first and last terms in Eq. A17 must balance. This implies that the dimensionless group multiplying the last term must be equal to one, which in turn determines $\dot{L}_s$:

$$\frac{k_G \alpha_G \omega_{1s}}{\rho_s \dot{L}_s} = \frac{k_G \alpha_G \omega_{10}}{\rho_0 \dot{L}_s} = 1 \Rightarrow \dot{L}_s = \frac{k_G \alpha_G \omega_{10}}{\rho_0} \tag{A21}$$

Initially the mass transfer will be confined to a solutal boundary layer near the upper interface having an instantaneous thickness δ that will be determined in the scaling analysis. At short contact times δ determines the length scale for the spatial derivatives; that is, $\hat{z}_s = \delta$. Once δ has penetrated the entire thickness of the liquid layer, the length scale for the spatial derivatives is determined by the dimensionless group appearing in Eq. A14; that is, $\hat{z}_s = L_0$. Since this is inherently an unsteady-state process, the appropriate time scale is the contact time t_c, which is any arbitrary time at which one chooses to observe the mass-transfer process; that is,

$$t_s = t_c \tag{A22}$$

To insure o(1) scaling the dimensionless group in Eq. A11 must be set equal to one, which then determines j_{1s}

$$\frac{D_{12}\omega_{1s}\rho_s}{\hat{z}_s j_{1s}} = \frac{D_{12}\omega_{10}\rho_0}{\delta j_{1s}} \Rightarrow j_{1s} = \frac{D_{12}\omega_{10}\rho_0}{\delta} \tag{A23}$$

This inherently unsteady-state process also dictates that the accumulation term balance the diffusion term (i.e., the first and third terms) in Eq. A10. This requires that the dimensionless group multiplying the accumulation term be set equal to one to insure o(1) scaling, which then determines the functional form of δ:

$$\frac{\rho_s \omega_{1s} \hat{z}_s}{t_s j_{1s}} = \frac{\delta^2}{t_c D_{12}} = 1 \Rightarrow \delta = \sqrt{D_{12} t_c} \tag{A24}$$

The implications of this time dependence for δ are the following for $\hat{z}_s$:

$$\begin{aligned} \hat{z}_s &= \delta \quad \text{for} \quad t_c < \frac{L^2}{D_{12}} \\ \hat{z}_s &= L_0 \quad \text{for} \quad t_c \geq \frac{L^2}{D_{12}} \end{aligned} \tag{A25}$$

To insure o(1) scaling the dimensionless group in Eq. A13 must be set equal to one, which then determines w_s:

$$\frac{\beta j_{1s}}{\rho_0^2 w_s} = \frac{\beta D_{12}\omega_{10}}{\rho_0 w_s \delta} = 1 \Rightarrow w_s = \frac{\beta D_{12}\omega_{10}}{\rho_0 \delta} \tag{A26}$$

Substitute these scale factors back into the dimensionless describing equations given by Eqs. A10–A17:

$$\rho^* \frac{\partial \omega_1^*}{\partial t^*} + \omega_{10}\mathrm{Bi}_\delta \rho^* \left(\frac{dL}{dt}\right)^* \frac{\partial \omega_1^*}{\partial \hat{z}^*} + \mathrm{Pe}\rho^* w^* \frac{\partial \omega_1^*}{\partial \hat{z}^*} = -\frac{\partial j_1^*}{\partial \hat{z}^*} \quad \text{for} \quad 0 \leq t_c < \frac{L^2}{D_{12}} \tag{A27a}$$

$$\frac{1}{\mathrm{Fo}} \rho^* \frac{\partial \omega_1^*}{\partial t^*} + \omega_{10}\mathrm{Bi}_L \rho^* \left(\frac{dL}{dt}\right)^* \frac{\partial \omega_1^*}{\partial \hat{z}^*} + \mathrm{Pe}\rho^* w^* \frac{\partial \omega_1^*}{\partial \hat{z}^*} = -\frac{\partial j_1^*}{\partial \hat{z}^*} \quad \text{for} \quad \frac{L^2}{D_{12}} \leq t_c < \infty \tag{A27b}$$

$$j_1^* = -\frac{\partial\left(\omega_1^* \rho^*\right)}{\partial \hat{z}^*} \tag{A28}$$

$$\rho^* = 1 - \mathrm{Pe}\left(\omega_1^* - 1\right) \tag{A29}$$

$$w^* = -j_1^* \tag{A30}$$

$$\omega_1^* = 1, \quad L^* = 1 \quad \text{at} \quad t^* = 0 \tag{A31}$$

$$j_1^* = 0 \quad \text{at} \quad \hat{z}^* = \frac{L_0}{\delta} L^* \tag{A32}$$

$$j_1^* = -\mathrm{Bi}_\delta \omega_1^* \left(1 - \omega_{10}\omega_1^*\right) \quad \text{at} \quad \hat{z}^* = 0 \quad \text{for} \quad 0 \leq t_c < \frac{L^2}{D_{12}} \tag{A33a}$$

$$j_1^* = -\mathrm{Bi}_L \omega_1^* \left(1 - \omega_{10}\omega_1^*\right) \quad \text{at} \quad \hat{z}^* = 0 \quad \text{for} \quad \frac{L^2}{D_{12}} \leq t_c < \infty \tag{A33b}$$

$$\rho^* \left(\frac{dL}{dt}\right)^* + \frac{1}{\omega_{10}} \frac{\mathrm{Pe}}{\mathrm{Bi}_\delta} \rho^* w^* = -\omega_1^* \quad \text{at} \quad \hat{z}^* = 0 \quad \text{for} \quad 0 \leq t_c < \frac{L^2}{D_{12}} \tag{A34a}$$

$$\rho^*\left(\frac{dL}{dt}\right)^* + \frac{1}{\omega_{10}}\frac{\mathrm{Pe}}{\mathrm{Bi}_L}\rho^* w^* = -\omega_1^* \quad \text{at} \quad \hat{z}^* = 0 \quad \text{for} \quad \frac{L^2}{D_{12}} \le t_c < \infty \tag{A34b}$$

Equations A27–A34 are those presented as Eqs. 20–27 in the body of this article. Scaling analysis implies that every term in each of the above equations will be bounded of o(1). Hence, if a dimensionless group is considerably larger than one, the dimensionless variable or derivative that this group multiplies must be much smaller than one to insure that the product is bounded of o(1).

Manuscript received Sep. 18, 2010, and revision received Mar. 16, 2011.